

Temperature-Dependent Anomalies in the Structure of the (001) Surface of LiCu_2O_2

Xuetao Zhu¹, Yangyang Yao¹, H. C. Hsu², F. C. Chou² and M. El-Batanouny¹

¹ *Physics Department, Boston University, Boston, MA 02215*

² *Center of Condensed Matter Sciences, National Taiwan University, Taipei 10617, Taiwan*

(Dated: November 1, 2018)

Surface corrugation functions, derived from elastic helium atom scattering (HAS) diffraction patterns at different temperatures, reveal that the Cu^{2+} rows in the (001) surface of LiCu_2O_2 undergo an outward displacement of about 0.15 Å as the surface was cooled down to 140 K. This is probably the first time that isolated one-dimensional magnetic ion arrays were realized, which qualifies the $\text{Li}^{1+}\text{Cu}^{2+}\text{O}_2^{2-}$ surface as a candidate to study one-dimensional magnetism. The rising Cu^{2+} rows induce a surface incommensurate structural transition along the a -direction. Surface equilibrium analysis showed that the surface Cu^{2+} ions at bulk-like positions experience a net outward force along the surface normal which is relieved by the displacement. Temperature-dependent changes of the surface phonon dispersions obtained with the aid of inelastic HAS measurements combined with surface lattice dynamical calculations are also reported.

PACS numbers: 68.35.B-, 68.35.Ja, 68.35.Rh, 68.49.Bc

Over the past decade LiCu_2O_2 has attracted considerable attention because it incorporates double-chain ladders of Cu^{2+}O , which makes it a prototypical quasi-one-dimensional quantum spin-1/2 magnetic system with competing magnetic interactions [1–4]. It still remains an exciting system since the recent discovery of ferroelectricity induced by an ordered helimagnetic phase, making LiCu_2O_2 the second cuprate to join the list of multiferroics [5–8]; LiCuVO_4 [9] being the first.

It was reported that LiCu_2O_2 exhibits a spin-singlet (or a gapped spin-liquid) ground state for temperatures $T > 30$ K [1]. Two successive magnetic phase transitions bring the system into an incommensurate long-range ordered state with a helicoidal spin structure in which the arms of the double-chain are antiferromagnetically ordered [3, 7, 8, 10–12]. The picture that emerges reveals the presence of a collinear sinusoidal spin-ordered phase, with spin polarization along the c -axis, below the transition temperature $T_N \simeq 24.6$ K. An initial modulation wave vector $\mathbf{Q} = (0, 0.172, 0)$ r.l.u. was reported, and was found to increase with decreasing temperature. At the second transition temperature $T_{FE} \simeq 23.0$ K, the spin polarization acquires small components along the a and b axes, giving rise to the helicoidal spin-ordered structure. This structure is characterized by an ellipse with the helical axis tilted by 45° from the b -axis within the ab plane, and with the incommensurate modulation still along the b -axis [10, 12]. \mathbf{Q} continues to increase and seems to saturate at $T \simeq 12$ K with $\mathbf{Q} = (0, 0.174, 0)$. The onset of the helicoidal phase induces ferroelectricity with polarization along the c -axis. Moreover, recent studies by resonant soft x-ray magnetic scattering [8] have demonstrated that the long-range ordered magnetic states are actually 2D-like ground states, where the 2D character was attributed to a small but effective spin coupling along the c -axis, which, in turn, suppresses quantum fluctuations. These measurements also revealed the presence of short-range spin correlations above T_N , which eventually

disappear at about 30 K leaving a spin liquid ground state at higher temperatures [8].

The onset of ferroelectricity below T_{FE} in LiCu_2O_2 was first reported by Park *et al.* [5]. Several models were proposed to explain the origin of electrical polarization in helicoidal magnetic systems. Two microscopic models were introduced to explain the mechanism responsible for multiferroicity in such systems, the first is based on the relation between the magnetoelectric effect and microscopic spin currents [13] and the second invoked the idea of inverse Dzyaloshinskii-Moriya [14]. In the former, the polarization is given by

$$\mathbf{P} \propto \mathbf{e}_{ij} \times (\mathbf{S}_i \times \mathbf{S}_j),$$

where \mathbf{S}_i and \mathbf{S}_j are the local spins at site i and site j respectively, and \mathbf{e}_{ij} is the unit vector connecting the i and j sites [13]. Subsequently, a phenomenological model based on electric polarization related symmetry-invariant Landau-Ginzburg terms of the form

$$\frac{\mathbf{P}^2}{2\chi_2} + \gamma \mathbf{P} \cdot [\mathbf{M} (\nabla \cdot \mathbf{M}) - (\mathbf{M} \cdot \nabla) \mathbf{M} + \dots]$$

was proposed [15]. In the case of LiCu_2O_2 all these models consistently support a spiral spin with components in the bc -plane, which agrees with the findings of Ref. [7, 8, 10–12].

Despite the extensive studies of bulk structural and magnetic properties of LiCu_2O_2 crystals cited above, to our knowledge, the only investigation of its surface properties was reported by the current authors [16], and involved helium atom scattering (HAS) studies of the structure and dynamics of the (001) surface of LiCu_2O_2 at room temperature. In that work, it was shown that the surface termination is exclusively a $\text{Li}^{1+}\text{Cu}^{2+}\text{O}_2^{2-}$ plane. In this letter we report a surprising discovery of temperature-dependent anomalies observed on this surface. For temperatures below 200 K, the Cu^{2+} rows were

found to rise above the surface plane; this, in turn, induces an incommensurate surface structure. As far as we know, this is probably the first time that an isolated one-dimensional row of magnetic ions was realized.

LiCu_2O_2 has a layered charge-ordered orthorhombic crystal structure belonging to the $Pnma$ space group. The primitive cell has lattice constants $a=5.73$, $b=2.86$, and $c=12.47$ Å. Single crystals of $\text{Li}_x\text{Cu}_2\text{O}_2$ with Li content of $x \sim 0.99 \pm 0.03$, which can be considered as stoichiometric LiCu_2O_2 , were grown by the floating-zone process [17]. The experimental setup and procedures of the HAS measurements are described in details in Ref. [16, 18].

In this work, we present surface diffraction patterns of the $\text{Li}^{1+}\text{Cu}^{2+}\text{O}_2^{2-}$ termination, obtained by the elastic HAS at temperatures below 210 K. Analysis of diffraction intensities yielded surface corrugations, which can be considered as direct pictures of the geometrical arrangement of the surface atoms [19]. As we previously reported [16], diffraction patterns recorded between room temperature and roughly 230 K showed none of the anomalies discussed below.

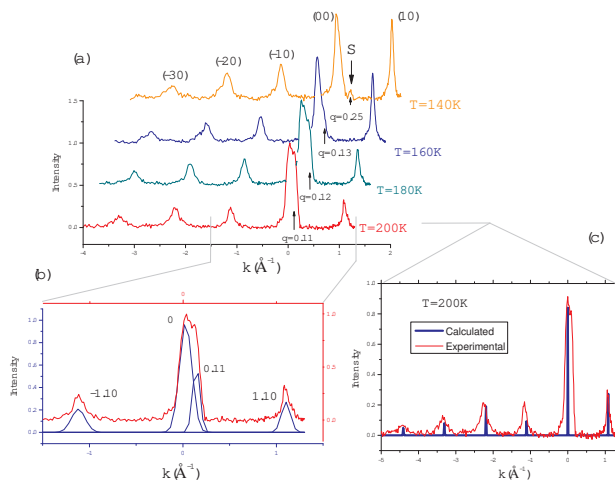


FIG. 1. (a) Diffraction patterns along the a -direction obtained at $T = 200, 180, 160$ and 140 K. Intensities are normalized to a specular intensity of 1. Arrows indicate the presence of satellite peak, denoted by S , at the specified wave vectors q . (b) Gaussian fit (blue) to experimental peaks obtained at 200 K. (c) Comparison between the measured diffraction peaks (red) and the calculated ones (blue). See text for details about the calculation.

LiCu_2O_2 samples were cleaved in situ, under ultra-high-vacuum conditions at $T = 200$ K. Subsequently, the samples were cooled down in steps to $T = 140$ K. Fig. 1(a) shows four diffraction patterns along the a -direction ((10) -direction) recorded at 200, 180, 160 and 140 K, respectively. It is clear that the intensity of the (10) first-order peak increases with decreasing temperature. Moreover, a shoulder is observed on the right side of the (00) specular peak at 200 K and progressively separates from it with decreasing temperature. A Gaussian fit to the

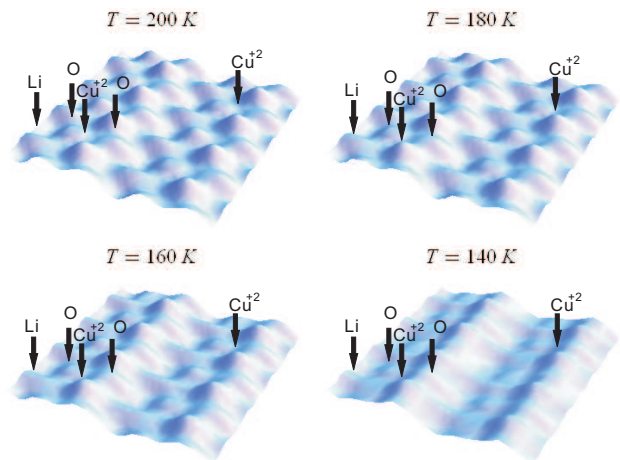


FIG. 2. Surface corrugations at different temperatures with T decreasing.

200 K diffraction peaks (DPs), Fig. 1(b), shows that the shoulder is actually a satellite peak at $\mathbf{q} = (0.11, 0)$ Å⁻¹. Similar fits to the DPs at lower temperatures show that \mathbf{q} increases monotonically with decreasing temperature to $\mathbf{q} = (0.25, 0)$ Å⁻¹ at 140 K. Henceforth, we denote this satellite peak by S . Further cooling to temperatures below 140 K showed no change in the diffraction pattern.

We used the *hard corrugated wall model* within the *eikonal approximation* to calculate the elastic scattering intensities and followed an iterative computational method to fit the calculated intensities to experimental measurements. Details of this iterative computational method can be found in Ref. [16] and references therein. Fig. 1(c) shows a very good match between the experimental diffraction pattern at 200 K (red curve) and the calculated intensities of the DPs (blue rods). An important product of this best fit is the topology of the primitive cell manifest in the two-dimensional surface corrugation function (SCF). The SCFs at $T = 200, 180, 160$ and 140 K are shown in Fig. 2, where the surface ion positions are indicated by arrows. It is clear from the SCFs that the Cu^{2+} ions rise monotonically with decreasing temperature. By calculating the difference between the maxima and minima of the SCFs, the largest displacement of the Cu^{2+} ions is estimated to be 0.14-0.15 Å above their bulk-like surface positions.

The presence of the satellite peak, S , is a manifestation of a surface incommensurate structure (SIS) along the a -direction. There can be two possible causes for the onset of the SIS: First, the appearance of surface electric dipoles associated with the elevation of the Cu^{2+} rows renders the surface unstable. Second, the tendency to maintain $\text{Cu}^{2+}-\text{O}^{2-}$ bond length close to its original value induces a lateral displacement of neighboring rows of O^{2-} ions toward the Cu^{2+} rows along the a -direction.

Fig. 3 shows five diffraction patterns along the a -direction sampled as the temperature was raised after

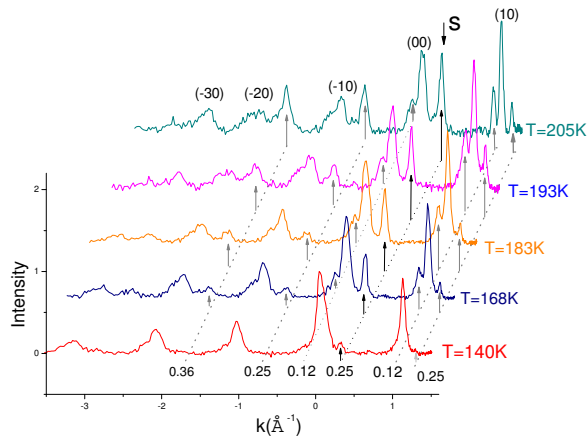


FIG. 3. Evolution of diffraction patterns along the a -direction with temperature increase above 140 K. Intensities are normalized to the specular intensity. Arrows mark satellite peak positions with their q values.

cooling to 140 K. A sequence of satellite peaks emerges, signaling the development of the SIS phases. The locations of these satellites are marked by arrows. The corresponding wave vectors, determined by Gaussian fits, are recorded next to each arrow. It should be noticed that the satellite intensities increase with increase in temperature, but their wave vectors remain constant. The emerging SIS is characterized by satellite wave vectors: $\mathbf{q} = (0.12 \pm 0.01, 0)$, $\mathbf{q} = (0.25 \pm 0.01, 0)$ and $\mathbf{q} = (0.36 \pm 0.02, 0) \text{ \AA}^{-1}$. An incommensurability close to $9/8$ was obtained by comparison with the commensurate first order wave vector of $\mathbf{q} = (1.10, 0) \text{ \AA}^{-1}$, in Fig. 1(b). All features associated with the incommensurate phase and the rise of the Cu^{2+} rows in the diffraction pattern completely disappear above 220 K.

Employing the approximate periodicity of $9/8$, we carried out a peak intensity fitting procedure similar to that described above. The resulting SCF is shown in Fig. 4. Moreover, we extracted the full-width-half-maximum (FWHM) of the specular peak from the diffraction patterns of Fig. 3; they are plotted in Fig. 5, together with the corresponding average domain size, as a function of temperature. The latter was obtained by deconvoluting the specular peak with an instrument transfer width [20] of $\Delta k_{inst} = 0.07 \text{ \AA}^{-1}$. It is clear from Fig. 3 and 5 that the incommensurate domains grow with rise in temperature.

In Fig. 6 we plot the intensity of the S -satellite peak at different temperatures, recorded during the cooling and heating segments of the experimental measurements. It is clear from Fig. 6 that the temperature dependence of the S -peak intensity displays a hysteresis loop with respect to the two segments of cooling and heating. The overall behavior points to a first-order commensurate-

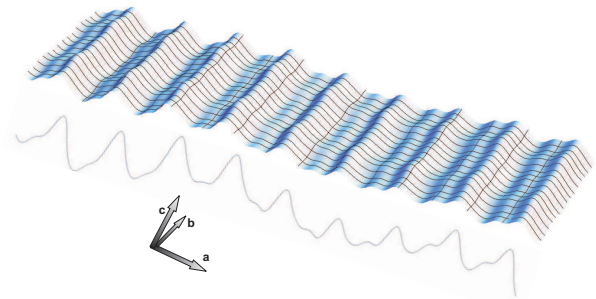


FIG. 4. Surface corrugation with a cross cut line for the incommensurate structure.

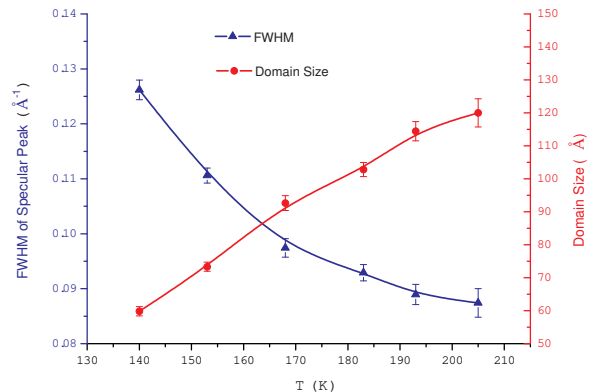


FIG. 5. Full-width-half-maximum (Δk) of the specular peak (blue), as well as the deconvoluted average domain size (red) as a function of temperature increase.

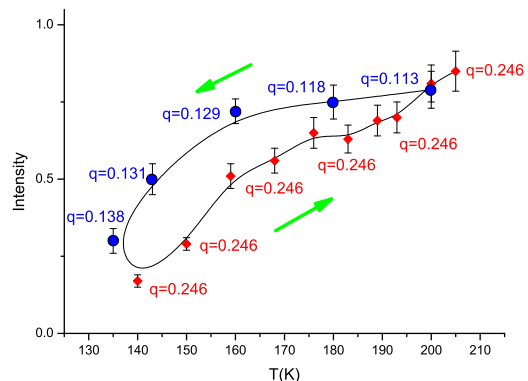


FIG. 6. The intensity of the S satellite peak. All intensities are normalized by setting the specular intensity to 1. The blue dots indicate the evolution of the corresponding q -vector with decreasing temperature. The red dots mark the evolution of the S -peak intensity at the saturated q -vector, as obtained upon heating. The black line is a guide to eye and green arrows show the temperature increasing or decreasing procedure.

incommensurate phase transition.

In order to understand the experimental observations

outlined above, we investigated the origin of the anomalous outward displacement of the Cu^{2+} rows with the aid of detailed surface equilibrium analysis [21]. This study showed that at bulk-like positions the surface Cu^{2+} ions experience a net outward force; and that this force can be relieved by displacing the Cu^{2+} rows outward from their bulk positions, along the surface normal [16].

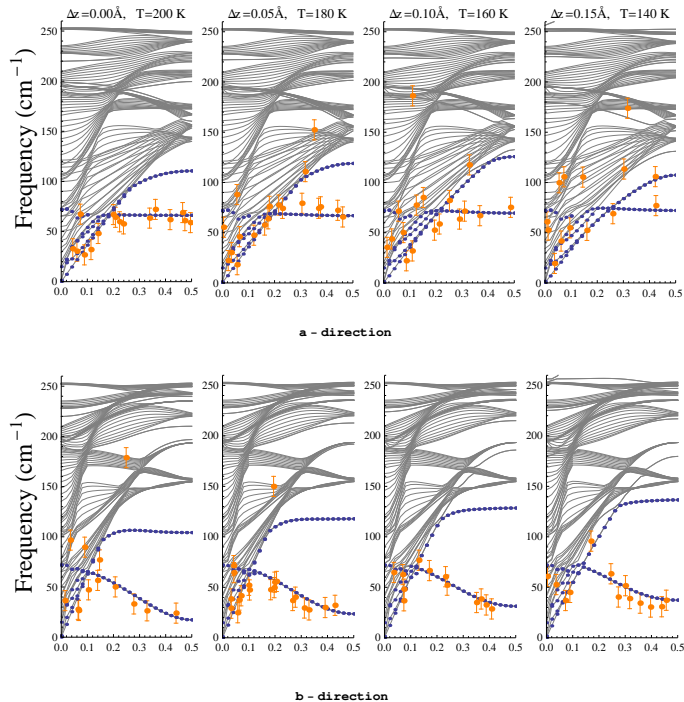


FIG. 7. Measured inelastic events (orange dots with error bars) reduced to the proper surface Brillouin zone (SBZ), as a function of decreasing temperature, superposed on calculated phonon dispersion curves corresponding to different surface Cu^{2+} displacements (Δz). The calculated surface phonon modes are indicated by blue dots, and the gray background represents the projection of the bulk bands on the SBZ. Upper panels: a-direction. Lower panels: b-direction.

Finally, we studied the changes in the surface phonon dispersion as a function of decreasing temperature. In these studies we employed inelastic HAS, together with lattice dynamical calculations based on a slab model with variable surface Cu^{2+} positions. The procedural details of these studies can be found in Ref. [16, 18]. Fig. 7 shows the results along high-symmetry directions - the experimental inelastic events are indicated by orange dots with error bars. The measurements were carried out at $T = 200, 180, 160$ and 140 K, and the surface phonon dispersion curves were calculated at different surface Cu^{2+} displacements from bulk-like positions, indicated by Δz , which were obtained from corresponding SCFs. As was reported in Ref. [16], the lowest two surface phonon dispersion branches (blue dots in Fig. 7) involve the motion of Cu^{2+} and Li^{1+} ions normal to the surface. We no-

tice the following trends with decrease in temperature: the lower branch along the b -direction displays a gradual increase in frequency close to the surface Brillouin zone (SBZ) boundary, while the slope of the upper branch and its SBZ frequency gradually decrease along the a -direction.

In summary, we presented experimental evidence that the Cu^{2+} rows in the (001) surface of LiCu_2O_2 undergo an outward displacement of about 0.15 \AA as the surface is cooled down to 140 K ; and that this displacement induces an incommensurate structure along the a -direction. The growth of the incommensurate domains was found to be thermally activated. The rise of the Cu^{2+} rows was supported by surface equilibrium analysis, which showed that the bulk-like positions experienced outward forces that were relieved by the displacement. Low-lying surface phonon branches, associated with the motion of Cu^{2+} and Li^{1+} ions normal to the surface, exhibit stiffening along the b -direction and softening along the a -direction as the temperature is lowered.

M. El-Batanouny acknowledges support from the U.S. Department of Energy under Grant No. DE-FG02-85ER45222. F. C. Chou acknowledges support from National Science Council of Taiwan under project No. NSC-95-2112-M-002. ME would like to thank C. Chamon and W. Klein for valuable discussions.

- [1] S. Zvyagin *et al.*, Phys. Rev. B **66**, 064424 (2002).
- [2] K.-Y. Choi *et al.*, Phys. Rev. B **69**, 104421 (2004).
- [3] T. Masuda *et al.*, Phys. Rev. Lett. **92**, 177201 (2004).
- [4] A. A. Gippius *et al.*, Phys. Rev. B **70**, 020406 (2004).
- [5] S. Park *et al.*, Phys. Rev. Lett. **98**, 057601 (2007).
- [6] H. J. Xiang and M.-H. Whangbo, Phys. Rev. Lett. **99**, 257203 (2007).
- [7] S. Seki *et al.*, Phys. Rev. Lett. **100**, 127201 (2008).
- [8] S. W. Huang *et al.*, Phys. Rev. Lett. **101**, 077205 (2008).
- [9] Y. Naito *et al.*, J. Phys. Soc. Jpn. **76**, 023708 (2007).
- [10] A. Rusydi *et al.*, Appl. Phys. Lett. **92**, 262506 (2008).
- [11] Y. Yasui *et al.*, J. Phys. Soc. Jpn. **78**, 084720 (2009).
- [12] Y. Kobayashi *et al.*, J. Phys. Soc. Jpn. **78**, 084721 (2009).
- [13] H. Katsura, N. Nagaosa, and A. V. Balatsky, Phys. Rev. Lett. **95**, 057205 (2005).
- [14] I. A. Sergienko and E. Dagotto, Phys. Rev. B **73**, 094434 (2006).
- [15] M. Mostovoy, Phys. Rev. Lett. **96**, 067601 (2006).
- [16] Y. Yao *et al.*, Surf. Sci. **604**, 692 (2010).
- [17] H. C. Hsu, H. L. Liu, and F. C. Chou, Phys. Rev. B **78**, 212401 (2008).
- [18] M. Farzaneh *et al.*, Phys. Rev. B **72**, 085409 (2005).
- [19] D. Farias and K.-H. Rieder, Rep. Prog. Phys. **61**, 1575 (1998).
- [20] R. L. Park, J. E. Houston and D. G. Schreiner, Rev. Sci. Instr. **42**, 60 (1971).
- [21] L. L. Boyer and J. R. Hardy, Phys. Rev. B **7**, 2886 (1973).